Available online at www.sciencedirect.com

ScienceDirect

Physics Procedia 00 (2009) 000–000

Physics Procedia

www.elsevier.com/locate/procedia

14th International Conference on Narrow Gap Semiconductors and Systems

# Spin dependent electronic structure and level crossings as a function of magnetic field in InAs nanowire

S.Q. Jin[a,b], J. Waugh[c,d], T. Matsuura[a,*], S. Faniel[c,*], H.Z. Wu[b] and Takaaki Koga[a,c,*,**]

[a]*Creative Research Institution Sousei Research Department, Hokkaido University, Sapporo, 001-0021, Japan*
[b]*Department of physics, Zhejiang University, Hangzhou, Zhejiang, 310027, China*
[c]*Graduate School of Information Science and Technology, Hokkaido University, Sapporo, 060-0814, Japan*
[d]*Department of physics, Virginia Polytechnic Institute and State University, Blacksburg, 24061, USA*

**Elsevier use only:** Received date here; revised date here; accepted date here

**Abstract**

We point out that the electric field formed in the surface inversion layer in InAs nanowires leads to effective magnetic fields, due to the Rashba effect, that are mostly aligned along the wire axis, *i.e.*, parallel to the external magnetic field *B*. While this situation leads to some similarities in spin splitting between the Zeeman and Rashba effects, extensive theoretical simulations revealed that large and small spin splittings should take place alternately at Fermi energies with increasing magnetic field *B*, as a result of the competition between the Rashba and Zeeman spin splittings. We suggest that an experimental detection of such characteristics should bring up quantitative insights into the relative strengths between the Rashba and Zeeman magnetic fields.
*PACS:* **71.28.+d**; 71.70.Ej;**72.25.-b**; 72.25.Dc; 72.80.Ey; 73.21.Fg; **73.23.-b**; 73.23.Ad; **73.63.-b**; 73.63.Nm

*Keywords:* spintronics; Rashba effect; AB effect; spin-orbit interaction; quantum wires; mesoscopic transport

In the field of spintronics [1,2], where semiconductors play a major role, spin physics is mainly studied through electrical transport and optical experiments. The development of nanowire technology is opening promising perspectives for future high-performance electronic devices [3]. Semiconductor nanowires typically belong to a new class of bottom-up fabricated nanoscale systems. Recent results have shown that nanowires can be of high crystalline quality and can have predefined lateral sizes down to 2 nm [4]. It is expected that cylindrical nano/microwires, that are made of semiconductors with surface accumulation layers such as in InAs [5], have an annular triangular potential well in the cross section around the wire surface; as a result, most of the electrons come to the wire surface and form a hollow cylindrical structure, as shown in FIG.1. If a uniform external magnetic field *B* is applied on the nanowire along the *z* axis, the magnetic flux will penetrate the cross section of the wire, and in consequence the magneto-conductance (MC) of the wire will oscillates with *B* due to the Aharonov-Bohm (AB) effect [6]. If a strong S.O. coupling such as the Rashba and Dresselhaus effects or the Zeeman effect is present, MC oscillations become aperiodic due to the spin splitting effect.

In this paper, we propose to use this aperiodicity in the AB oscillations to obtain insight towards quantitative understanding of the spin-orbit coupling constants. In experiments using two-dimensional electron gas systems, the

*This work is supported by KAKENHI, Grant-in-Aid for Young Scientists (A), No. 19684009. Grant-in-Aid for JSPS fellow and financial support from Iketani Science and Technology Foundation are highly acknowledged.
** Corresponding author. Tel.: +81-11-706-6538; fax: +81-11-706-7803. E-mail address: koga@ist.hokudai.ac.jp.

spin splitting values can be evaluated by Shubnikov-de Haas beating [7], weak localization/anti-localization [8] or spin interference [9], but none of them provide a sufficient tool for quantitative determination of the spin-orbit (S.O.) coupling constants. We will consider a ballistic cylindrical wire made of InAs with radius $R$. Intuitively, the Rashba effect can be explained as a Zeeman effect for a moving electron in an asymmetric confinement potential, where a moving electron, with a velocity $\mathbf{v}$, feels an *effective* magnetic field $\mathbf{B}_{\text{eff}}$ whose direction is in $\mathbf{v}\times\mathbf{E}_{\text{QW}}$. Here, the electric field $\mathbf{E}_{\text{QW}}$ is given as a derivative of the confinement potential. In InAs nanowires, $\mathbf{E}_{\text{QW}}$ in the surface inversion layer is centripetal due to the annular triangular potential well around the wire surface. The momentum of the electron can be decomposed into $\mathbf{k}_{\parallel}$ and $\mathbf{k}_{\perp}$, parallel and perpendicular to the wire axis, respectively, where $\mathbf{k}_{\perp}$ represents a momentum around the wire surface, *i.e.*, an angular momentum. It is noteworthy that $\mathbf{k}_{\perp}$ couples with both the external magnetic field $\mathbf{B}$ and $\mathbf{B}_{\text{eff}}$ via the Zeeman and Rashba effects, respectively, where $\mathbf{B}$ and $\mathbf{B}_{\text{eff}}$ are parallel to each other. We find two quantum numbers in this system, namely, $m$ and $n$, where $m$ is the quantization due to the radial confinement and $n$ is the angular momentum quantization associated with $\mathbf{B}$ (via $\mathbf{k}_{\perp}$). Note that $m$=0, 1, 2, … and $n$=0, ±1, ±2, …. Therefore, the energy subband levels can be marked by $(n, m)\uparrow,\downarrow$, where ↑ and ↓ denotes the spin up and down states, respectively. Besides, the fact that $\mathbf{B}$ and $\mathbf{B}_{\text{eff}}$ are in the same orientation makes some characteristics in the spin splitting similar between the Zeeman and Rashba effects, *i.e.*, they give a shift to the AB oscillations which can be considered as the origin of the aperiodicity. Detailed studies of such aperiodicity would provide useful insights into quantitative understanding of the Rashba and Zeeman effects.

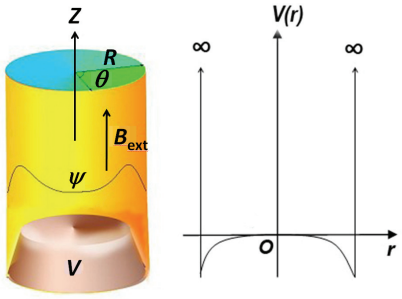


FIG. 1 Schematic picture of cylindrical nanowire system and a cross-sectional potential diagram, where $O$ indicates the reference of the energy.

Because of the translational invariance and cylindrical symmetry of the ballistic wire, it is convenient to expand the one-electron wave function [6] as $\psi = e^{ik_z z}\sum_n e^{in\theta}\varphi_n(r)$ with a momentum component $k_z$ along the wire axis. $\varphi_n(r)$ is the radial-position-dependent spinor for a given orbital angular momentum $n$ about the wire axis. In the presence of an external uniform magnetic field, the diagonal elements of the translationally invariant Hamiltonian is given as

$$H_{nn} = -\frac{\hbar^2}{2m^*(r)}\left[\frac{\partial^2}{\partial r^2}+\frac{1}{r}\frac{\partial}{\partial r}-\frac{n^2}{r^2}-k_z^2+m^*(r)\left(\frac{\partial}{\partial r}\frac{1}{m^*(r)}\right)\frac{\partial}{\partial r}-\frac{eB}{\hbar}n-\frac{e^2B^2}{4\hbar^2}r^2\right]+V(r)+\alpha(r)\left(\frac{n}{r}+\frac{eBr}{2\hbar}\right)-\frac{1}{2}g^*\mu_B B. \quad (1)$$

Then the off-diagonal elements of $H$ are $H_{n,n-1}=-i\alpha(r)k_z$ and $H_{n,n+1}=i\alpha(r)k_z$, which mix different orbital angular momenta $n$ and $n'$ due to the spin-orbit interaction, where the form of $\alpha(r)$ is found in Refs. 6 and 8.

We first point out that the Hamiltonian for the Rashba effect from $\mathbf{E}_{\text{QW}}$ couples nicely with the electron's angular momentum states. The annular potential inside the wire is obtained by the self-consistent procedure, solving the Poisson and Schrödinger equations self-consistently. After solving $H\psi(r,\theta,z) = e^{ik_z z}\sum_n e^{in\theta}\sum_{n'} H_{nn'}\varphi_{n'}(r)$, the energy eigenvalues and eigenvectors are acquired, and then the corresponding Fermi energy and the density of states are found, which are used to calculate the new charge distribution $\rho(r)$. $\rho(r)$ is then plugged back into the Poisson equation to find a new potential $V(r)$, the same procedure is enforced until $V(r)$ converges. The interaction elements are neglected in this self-consistent calculation since they are sufficiently small compared to the diagonal elements. After obtaining the converged $V(r)$, the Fermi energy is calculated taking $H_{n,n-1}$ and $H_{n,n+1}$ into account.

$$E_F = \frac{E^{\downarrow}_{m,n-1}(0)+E^{\uparrow}_{m,n}(0)}{2} \pm \frac{1}{2}\sqrt{\left(E^{\downarrow}_{m,n-1}(0)-E^{\uparrow}_{m,n}(0)\right)^2+\langle\alpha\rangle^2 k_F^2}+\frac{\hbar^2 k_F^2}{2m_z^*}, \quad (2)$$

where $\langle\alpha\rangle^2 = \left|\langle m,n-1,\downarrow|\alpha(r)|m,n,\uparrow\rangle\right|^2$ and $\alpha(r) = \frac{\hbar^2 E_P}{6m_e}\frac{\partial}{\partial r}\left(\frac{1}{E-V(r)+E_g+\Delta_{so}}-\frac{1}{E-V(r)+E_g}\right)$. (3)

$E_{m,n}^{\uparrow\downarrow}(0)$ denotes the energy level with $k_z$=0. For each coupled state $i$ [$i$=($m$, $n$)↑ or ($m$, $n$-1)↓], the Fermi wavevector $k_F$ is associated with the number of electrons in the pertinent subband $N_i$ by $N_i=k_F L/\pi$, where $L$ is the length of the wire. Thus, the Fermi energy can be attained by solving $\Sigma N_i(E_F)=N_{tot}$, $N_{tot}$ being the total number of the electrons.

We then calculate the crossings of the electronic energy levels for all the one-dimensional angular momentum states as a function of magnetic field. In order to make the annular potential well similar to a triangular potential well in the surface accumulation layer, we chose a carrier density small enough to keep most of the electrons at the lateral surface of the wire. The electron density in this surface accumulation layer, when converted to the sheet carrier density $N_S$, should be around $10^{16}$ m$^{-2}$ as in the surface accumulation layer of bulk InAs single crystals.[5]

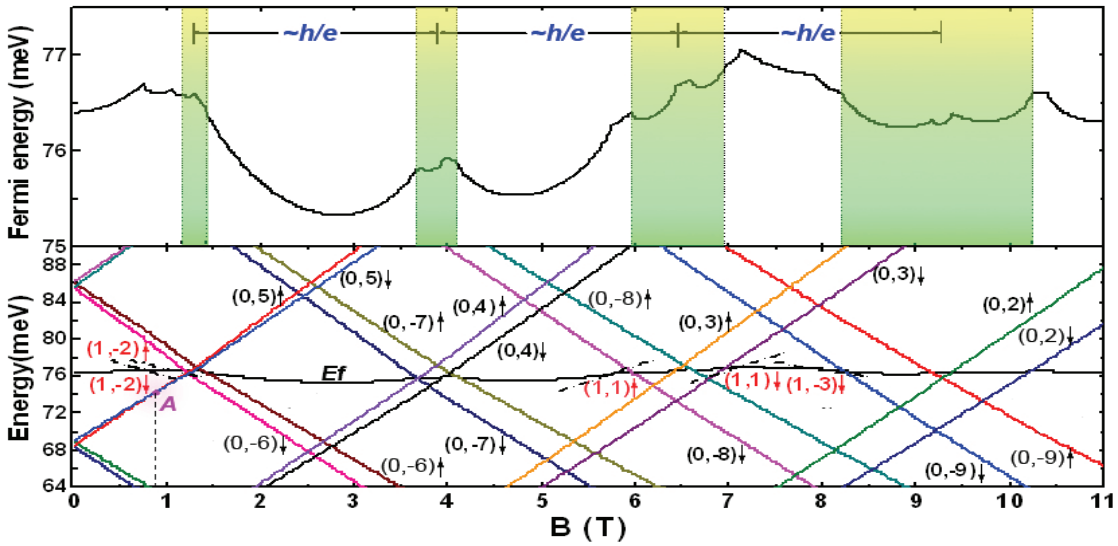


FIG. 2 Lower panel: The calculated first subband energy levels ($m$=0) for an InAs nanowire (60 nm in diameter) as a function of magnetic field along the wire. The crossing points by various angular momentum states with subband index due to the radial confinement $m$=1 are indicated by black dash lines. Upper panel: Zoom-in section of the Fermi energy as a function of $B$. The clusters of the crossings with $m$=0 distribute in the yellow-green shaded regions. The distance between the middle lines of two yellow-green regions is $h/e$ in magnetic flux.

We studied the subband and the Fermi energy levels as a function of magnetic field in two kinds of InAs nanowire with radius $R$=60 nm and 100 nm, respectively. The effective mass ($m^*$) and the $g$-factor ($g^*$) of InAs in Eq. (1) are set to be $0.023m_e$ and -14, respectively. Parameter values $E_P$=21.5 eV and $\Delta_{so}$=0.39 eV are used in Eq. (3). Our results showed that the crossing points at which the subband energy levels cross the Fermi energy have a quasi-periodic distribution as a function of $B$. However, in a closer look, the distribution is aperiodic due to the Zeeman and Rashba splittings. For higher carrier densities, the crossing points due to the higher radial subbands ($m\geq1$) appear which complicate the quasi-periodic energy diagram.

**a. 60 nm wire**

We first studied a nanowire with a diameter of 60 nm, where the 3-dimensional (3D) average carrier density within the nanowire is $5\times10^{23}$ m$^{-3}$, equivalent to $0.75\times10^{16}$ m$^{-2}$ in $N_S$ using 60 nm for the diameter. FIG. 2 illustrates the subband energy levels near the Fermi energy as a function of $B$. It is shown that the energies for the states with positive (negative) angular momentum subband index $n$, increase (decrease) with increasing $B$. This results in many crossing points between the spin-split quantized energy levels and the Fermi energy as a function of $B$. Though these crossing points take place mostly periodically with $B$, consistent with the $h/e$ flux quantization as shown in the upper panel of FIG. 2, they are, more precisely, aperiodic due to the Rashba and Zeeman spin splittings as well as due to the crossing of the subband energies from the $m$=1 states.

The upper panel in FIG.2 indicates the Fermi energy as a function of $B$, which exhibits singularities at each crossing point. The Zeeman splitting becomes the dominant spin-splitting mechanism at large $B$'s. So the effect of the Rashba effect can be seen only in relatively low $B$'s, where $B$ is equivalent to $B_{\text{eff}}$. It is worth mentioning that in the states with positive (negative) $n$ values, the electrons move in a counter-clockwise (clockwise) direction in the annular potential well when $k_z$ is small, therefore $\boldsymbol{B}_{\text{eff}}$ is parallel (antiparallel) to the external $\boldsymbol{B}$. The spin splitting is diminished (enhanced) by the interplay between the Zeeman and Rashba effects in a positive (negative) $n$. At the point $A$ ($B$=0.97 T) in the lower panel of FIG.2, the spin splitting is zero in the state (0, 5) due to the competition between Zeeman and Rashba effect. On the other hand, in the state (0, -6), a finite spin splitting energy found at $B$=0 just increases with $B$ monotonically.

**b. 100 nm wire**

In order to observe crossing points at lower $B$'s, which is a more favored situation in experiment, we also investigated a wire with the diameter 100 nm, the 3D carrier density was set to be $2\times10^{23}$ m$^{-3}$, equivalent to $0.5\times10^{16}$ m$^{-2}$ in $N_S$ using 100 nm for the diameter. FIG.3 shows the crossing levels in this wire. It is seen that the spin splittings in positive $n$'s are much smaller than those in negative $n$'s. This means that small and large spin

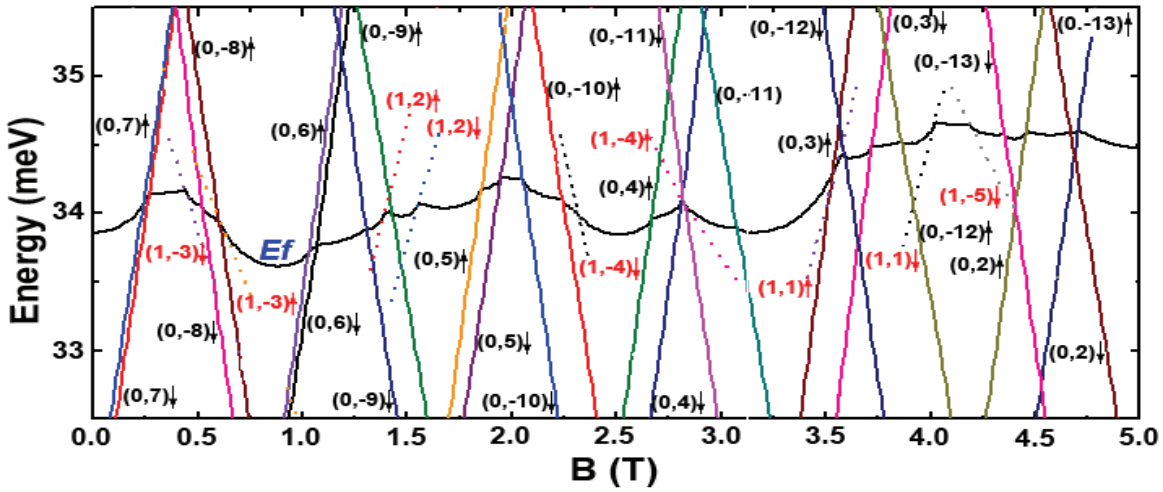


FIG.3 Energy level structure near Fermi energy for 100 nm wire with 3D $N_{3D}$=2×10$^{23}$ m$^{-3}$.

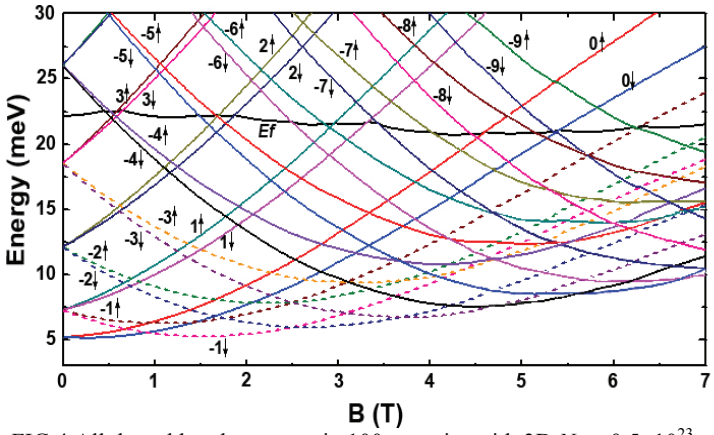


FIG.4 All the subband structure in 100 nm wire with 3D $N_{3D}$=0.5×10$^{23}$ m$^{-2}$.

splittings take place alternately with increasing $B$, at the crossing points with the Fermi energy. When the 3D carrier density is reduced to be $0.5\times10^{23}$ m$^{-3}$, the higher subbands ($m\geq1$) completely disappear below the Fermi energy (see FIG.4), so the crossing points become more periodic and they are only influenced by the Rashba and Zeeman spin splittings. Because the carrier density is quite small, the Fermi energy is close to relatively low angular momentum states ($n$=0, ±1, ±2, ±3) with subband index $m$=0. These small $n$ states, but with negative $n$ values ($n$<0), go down with increasing $B$ at relatively small $B$'s and then bend back to the Fermi energy at high $B$'s as shown in FIG.4. These energy levels indicated by dashed curves in FIG.4, where the subband energy levels are marked as $n\uparrow,\downarrow$. It is noted that the carrier density inside the wire can be controlled by gate which surround the nonowire. The aperiodicity in the crossing points can be better studied by plotting the crossing points on a $V_g$-$B$ plane (or $N_{tot}$ -$B$ plane), which would more clearly illustrate the spin splittings of the crossing points from the experimental point of view.

## References


[1] S. A. Wolf, D. D. Awschalom, R. A. Buhrman, J. M. Daughton, S. von Molnar, M. L. Roukes, A. Y. Chtchelkanova, D. M. Treger, Science **294**, 1488 (2001).

[2] I. Zutic, J.Fabian, and S. Das Sarma, Rev. Mod. Phys. **76**, 323 (2004).

[3] S. Roddaro, K. Nilsson, G. Astromskas, L. Samuelson, L.-E. Wernersson, O. Karlstrom, and A. Wacker, Appl. Phys. Lett. **92**, 253509 (2008).

[4] M. T. Björk, B. J. Ohlsson, T. Sass, A. I. Persson, C. Thelander, M. H. Magnusson, K. Deppert, L. R. Wallenberg, and L. Samuelson, Nano Lett. **2**, 87 (2002).

[5] T. Matsuyama, R. Kürsten, C. Meißner, and U. Merkt, Phys. Rev. B **61**, 15588 (2000).

[6] Yaroslav Tserkovnyak, and Bertrand I. Halperin, Phys. Rev. B **74**, 245327 (2006).

[7] J. Nitta, T. Akazaki, H. Takayanagi and T. Enoki, Phys. Rev. Lett. **78**, 1335 (1997).

[8] T. Koga, J. Nitta, T. Akazaki, and H. Takayanagi, Phys. Rev. Lett. **89**, 046801 (2002).

[9] T. Koga, Y. Sekine, and J. Nitta, Phys. Rev. B **74**, 041302(R) (2006); T. Koga, J. Nitta, and M. van Veenhuizen, Phys. Rev. B **70**, 161302(R) (2004).